Science Bulletin 64 (2019) 1336–1347

Contents lists available at ScienceDirect

Science Bulletin

journal homepage: www.elsevier.com/locate/scib

Review

Recent progress of nanogenerators acting as biomedical sensors *in vivo*

Jinyan Sun [a,1], Anping Yang [a,1], Chaochao Zhao [b,1], Fang Liu [a], Zhou Li [b,c,*]

[a] Department of Biomedical Engineering, School of Medical Engineering, Foshan University, Foshan 528000, China
[b] Beijing Key Laboratory of Micro-Nano Energy and Sensor, Beijing Institute of Nanoenergy and Nanosystems, Chinese Academy of Sciences, Beijing 100083, China
[c] Center on Nanoenergy Research, School of Physical Science and Technology, Guangxi University, Nanning 530004, China

ARTICLE INFO

Article history:
Received 18 April 2019
Received in revised form 31 May 2019
Accepted 17 June 2019
Available online 3 July 2019

Keywords:
Nanogenerator
Implantable device
Biomedical sensor
In vivo

ABSTRACT

Since the nanogenerator (NG) was invented in 2006, it has been successfully developed and utilized to harvest various forms of mechanical energy *in vivo*. The NGs promote the progress of self-powered biomedical devices. Moreover, NGs can also be used as sensors to detect a variety of important physiological signals, which brings us closer to real-time, high-fidelity monitoring of physical and pathological information. This paper summarizes the *in vivo* applications of NGs as biomedical sensors, including in cardiac sensors, respiration sensors, blood pressure sensors, gastrointestinal sensors and bladder sensors. However, there are still many challenges in using NGs as sensors *in vivo*. For example, how can we minimize and encapsulate the NGs, how can we increase the stability and reliability during long-term detection, and how can we establish a corresponding relationship between the NG's electrical output and the physiological signals. It is also critical to follow the medical principles more closely in the development of self-powered sensors in the future. We believe that the self-powered sensors would promote the development of the next-generation healthcare monitoring systems.

1. Introduction

Implantable electronic medical devices (IEMDs) have experienced rapid development in recent decades, allowing them to more effectively enhance the quality of patients' lives, and prolong patients' lifespan. With the continuous development of medical technology, medical devices for the diagnosis and detection of various diseases are increasing [1–3]. IEMDs, such as cardiac pacemakers, cerebral pacemakers and nerve stimulators, provide the functions of disease monitoring and targeted treatment. However, their development still faces many challenges, such as how to minimize size and reduce weight. Another burning problem is the power supply of IEMDs. For example, the pacemaker invented by Wilson Greatbach was implanted into human body in 1960, which had a working life of less than two years. The zinc-oxygen battery had obvious shortcomings, such as poor sealing and current leakage [4,5]. In 1972, Italian scientists applied lithium batteries to implantable medical devices. With the continuous improvement of lithium battery technology, the life of the lithium battery inside a cardiac pacemaker can reach about 10 years. This progress has been recognized by the medical industry and patients. In addition to research on lithium batteries, researches on biofuel cells [6,7] and nuclear batteries [8–10] are also deepening. However, the battery of the IEMD has a common shortcoming: the battery life is limited. After the batteries are depleted, they need to be replaced by surgery, which undoubtedly increases the risk of infection and death as well as the economic burden to the patients. Replacements take over about 25% of all implantation procedures, due to battery depletion [11]. Therefore, the self-powered IEMDs have attracted extensive attention, and have become a research hotspot [12].

No external power supply is necessary for self-powered IEMDs during their work and function. Because the battery takes up most of the size and weight of IEMDs, the self-powered system can greatly promote the miniaturization and weight reduction of the IEMDs. There are a variety of energy sources in human body, and many ways are established to harvest chemical energy, thermal energy, electrical energy and mechanical energy [13,14]. Among all these forms of *in vivo* energy, biological mechanical energy is regarded as the most sufficient and common energy. The biological energy produced by human movements (including physical movements, contractions/relaxations of the lung, heart, muscles and blood circulation, etc.) can be used effectively [15]. Zhong Lin Wang's group [16] firstly invented piezoelectric nanogenerator (PENG) of zinc oxide nanowire arrays in 2006, which could convert the environmental mechanical energy into electrical energy

* Corresponding author.
E-mail address: zli@binn.cas.cn (Z. Li).
[1] These authors contributed equally to this work.

https://doi.org/10.1016/j.scib.2019.07.001
2095-9273/

through piezoelectric effect. In 2012, his group firstly invented triboelectric nanogenerator (TENG) [17]. TENG could achieve rapid conversion of mechanical energy into electric energy via the coupling of the triboelectric effect and the electrostatic induction between two contacted materials. PENG and TENG have become the most promising biomechanical energy harvesting devices since their invention, providing a huge space for the development of self-powered IEMDs [18].

Since its inception, the design of PENG has developed from the original ZnO nanowires, nanocomposite ($BaTiO_3$ or $ZnSnO_3$) to inorganic films, for example, lead-free $NaKNbO_3$, $(1-x)Pb(Mg_{1/3}Nb_{2/3})O_{3-x}PbTiO_3$ (PMN-PT), poly (vinylidenefluoride-*co*-trifluoroethylene) (PDFV-TrFE), $Pb(Zr_xTi_{1-x})O_3$ (PZT), and polyvinylidene fluoride (PVDF) [19–23]. These improvements help achieve high output power, good stability, and commendable safety for PENG. In addition, the output power and stability of TENG are being constantly improved through the innovation of the materials' type and morphology, new designs of the structure, and the utility of hybrid devices [24–27]. PENG and TENG have provided tremendous potentials to harvest *in vivo* biomechanical energy. Our group [28] developed an implantable PENG based on a single ZnO nanowire, which could harvest the mechanical energy generated by heartbeat and breathing in living rats. This is the first time that PENG had been used to harvest biomechanical energy *in vivo*. In 2014, Zheng et al. [29] designed a TENG that could harvest the mechanical energy from a rat's normal breathing, convert the harvested energy into electrical energy and successfully drive a pacemaker to regulate a rat's heart rate (HR). This group [30] then implanted the encapsulated TENG into small pigs to harvest the mechanical energy of heartbeat, achieving the leap from using TENG to harvest biomechanical energy from small to large animals.

PENG and TENG can not only harvest mechanical energy in living bodies, which provides new options for IEMDs driven by self-powered systems [24,31], but they can also serve as sensors to detect vital signs, such as HR and breathing [32,33]. NGs with a sensor function provide a new promising way to diagnose and treat diseases, and expand the application range of IEMDs. In this review, we first briefly introduce the principle of NGs and then focus on the applications of NGs as biomedical sensors *in vivo*. In addition, we discuss the remaining challenges of NG-based self-powered systems. Finally, a summary and a prospect of the development of NGs in the future are carried out. This review could promote the future evolution of NGs as *in vivo* sensors in daily life and in clinic.

2. Working mechanism of NG

Maxwell's displacement current theory is the theoretical source of NGs [34]. Taking TENG as an example, it is usually composed of two electrodes and at least one pair of triboelectric layers. The displacement current is generated from the horizontal/vertical movement of the layers with opposite triboelectric charges. Under external force, these charges can lead to a time-varying electric field. Then a related electric flux changes over time. This will result in a generation of displacement current between the two electrodes of TENGs [35]. After more than ten years of development, many types of NGs have been developed to act as biomedical sensors *in vivo*.

2.1. PENG

PENG contains an insulator piezoelectric material with the top and bottom electrodes covered on its two surfaces. Its working mechanism relies on the piezoelectric potential, which occurs due to the presence of electric dipoles generated in the materials under straining. The electric dipole can be induced by the separation of the positive and negative charge centers of the lattice, or carried by molecular groups (such as sucrose) directly. Increased stress leads to higher polarization charges. The electrostatic potential caused by the polarization charges is balanced by the flow of electrons from one electrode to the other through external load. For example, in general, the centers of positive ion and negative ion are matched with each other in wurtzite-structured ZnO nanowire. When dynamic force stress is applied, the charge centers are dislocated and a piezoelectric potential is generated. Once the deformable ZnO is connected to an external circuit containing a load, the electrons will flow through it in order to balance the potential difference (Fig. 1a, b) [36]. Ever since PENG was designed by Zhong Lin Wang's group [16] in 2006, the principle of PENG has been clarified by a large number of following research works and a wide variety of flexible PENGs have been successfully developed (Fig. 1c).

2.2. TENG

TENG is based on the coupling of triboelectric effect and electrostatic induction between two contacted materials. The triboelectric effect is a charging effect caused by contact. It states that when two materials come into contact, chemical bonds are formed between the surfaces of these two materials, and charge moves from one material to the other due to their different abilities to capture electrons. The transferred charge may be electrons, ions or molecules. When the two materials are separated, some of the bonding atoms tend to retain excess electrons, and some tend to lose electrons, thus a potential difference induced by triboelectric charges drives electrons to flow between the top and bottom electrodes on the two materials' surfaces [37]. Based on this principle, TENG can be divided into four types: single-electrode mode, freestanding triboelectric-layer mode, lateral sliding mode and vertical contact-separation mode (Fig. 2) [13]. The single electrode mode is designed for harvesting energy from a free object without connecting lead. The freestanding triboelectric-layer mode is introduced for generating power between two electrodes. The lateral sliding mode utilizes lateral direction polarization of two dielectrics. The vertical contact-separation mode employs the vertical polarization. Due to the movement pattern of organs and optimal fitting mode between devices and organs, the vertical contact-separation mode is most commonly used in the present *in vivo* sensors. Any two materials with different electron releasing and donating abilities can be used in the manufacture of TENG, which allows more materials to be used as TENG's friction materials, thus expanding the application field of TENG [38].

With the continuous development of PENG and TENG, NGs have been successfully used to harvest various types of biomechanical energy from living bodies, such as the breathing of the mouse [28], heartbeat of the mouse/pig/bovine/ovine [28,33,39], the movement of diaphragm and lung of the bovine and ovine [39], the pulsation of the pig [19], the gastrointestinal movement of the pig [40] and so on. The output power generated by NGs is high enough to drive small-sized, low-power electronic devices such as LEDs and wireless transmitters [24,33]. This provides huge potential for the development of self-powered IEMDs and the applications of using NGs as biomedical sensors.

3. NG as biomedical sensors

As a new power generation technology, NGs are able to convert biomechanical energy into electrical energy. Based on this, NGs can also be used as sensors to obtain information on the biomechanical input by analyzing the output electrical signals. Herein, we focus

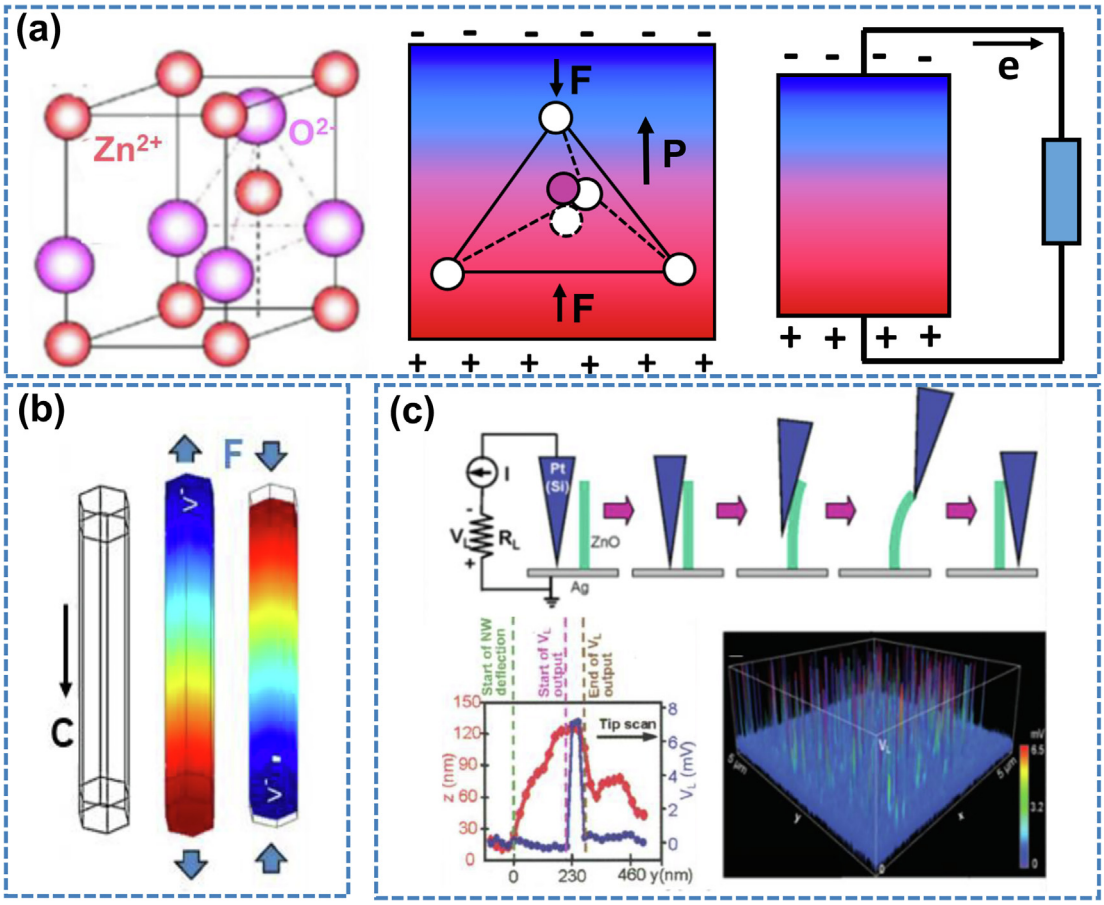

Fig. 1. (Color online) Working principle of PENG. (a) Atomic model of ZnO with wurtzite-structure and the principle of the piezoelectric effect. (b) Numerical calculation of the piezoelectric potential distribution in a ZnO nanowire under axial strain. (c) Atomic force microscope (AFM) drives a single nanowire to generate an electrical output.

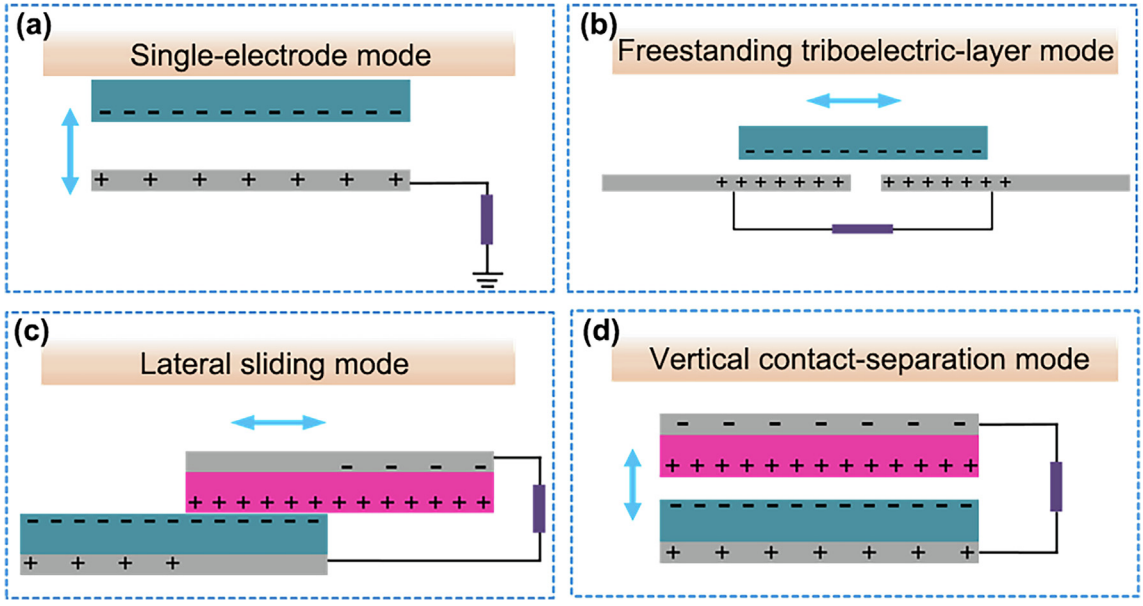

Fig. 2. (Color online) The four fundamental modes of TENGs. (a) Single-electrode mode. (b) Freestanding triboelectric-layer mode. (c) Lateral-sliding mode. (d) Single-electrode mode.

on a review of NG-based *in vivo* sensors, which include the material, structure and performance of the sensors, *in-vitro* simulation, and *in-vivo* application.

3.1. Cardiac sensor

Liu et al. [41] developed a self-powered endocardial pressure sensor (SEPS). The SEPS was based on an implantable TENG (iTENG), and consisted of the triboelectric layers, electrode layers, spacer layers and encapsulation layers. A nano-polytetrafluoroethylene (PTFE) film (25 μm) was employed as one triboelectric layer. An ultrathin Au layer (50 nm) on the back of the nano-PTFE film was used as an electrode. The other triboelectric layer and electrode was an Al foil with the thickness of 100 μm (Fig. 3a). Corona discharge process was carried out in the preparation of PTFE triboelectric layer. After a regular external mechanical force was applied *in vitro*, the open circuit voltage (V_{oc}) was up to about 6.2 V. By mimicking the change of endocardial pressure (EP) by modulating the pressure in a confined chamber with a gas control unit, the voltage generated by SEPS in the chamber increased correspondingly when the pressure varied from 70 to 350 mmHg. Specifically, the values of voltage peaks showed excellent linearity with the external pressures ($R^2 > 0.99$), with a high sensitivity of 1.2 mV/mmHg (Fig. 3b). The miniaturized device (1 cm × 1.5 cm × 0.1 cm) was implanted into the left ventricle of a male adult Yorkshire pig (40 kg). The voltage outputs of SEPS were highly synchronous to the femoral arterial pressure (FAP). The V_{oc} was about 80 mV at rest (systolic FAP < 100 mmHg), and increased simultaneously along with augment of FAP from 90 to 180 mmHg at the arousing stage (Fig. 3c). What's more, there was a remarkable linearity between SEPS voltage peaks and FAP ($R^2 = 0.974$) (Fig. 3d). Based on the simulation results *in vitro*, pressure inside left ventricular (P_{LVP}) could be obtained: P_{LVP} (mmHg) = 1.195U (mV). This calculated P_{LVP} kept pace with FAP modulated by epinephrine. Besides, the left atrial pressure (LAP) could also be monitored by implanting SEPS into the left atrial. The V_{oc} peak was about 8 mV when HR was 114 bpm and FAP was 92/70 mmHg. When FAP arose from 110 to 176 mmHg after epinephrine injection, the V_{oc} peak synchronously decreased from 8 to 5.5 mV. When ventricular premature contraction was modeled, a remarkable increase appeared in V_{oc} at the left atrial, which temporally coincided with the abnormal R wave in ECG. The rhythm and amplitude of output voltage could give indication for arrhythmias together. The encapsulated device showed excellent blood compatibility and outstanding long-term reliability, which met the application requirements *in vivo*.

Kim et al. [33] developed a flexible 0.5 mol% Mn doped single-crystalline 0.4 $Pb(Mg_{1/3}Nb_{2/3})O_3$-0.6 $Pb(Zr_{0.42}Ti_{0.58})O_3$ (PMN-PZT-Mn) based PENG. The packaged device was sutured onto the epicardium in a male adult Yorkshire porcine model (40 kg). The harvesting device produced a V_{oc} of 40 V and a short-circuit current (I_{sc}) of 4.5 μA through mechanical bending and unbending deformations on a linear stage at a frequency of 0.4 Hz. In addition, the PENG could work at various frequencies (1.7, 2.7, 5.3 Hz). The PENG generated a V_{oc} of 17.8 V and an I_{sc} of 1.75 μA from the *in vivo* contraction and relaxation motion of the porcine heart. It was important to emphasize that the generated electrical signals were well consistent with the electrocardiogram (ECG) (Fig. 4a). All clear characteristic waves in ECG (T, QRS and P waves) could be revealed in generated current signal of PENG (Fig. 4b). The cell viability test showed that this PMN-PZT-Mn NG had no detectable cytotoxicity to mouse cardiac muscle cell line (HL-1), human embryonic kidney cells (HEK293), and rat cardiomyoblasts (H9C2) after 5 days of culture. Moreover, the device led to little

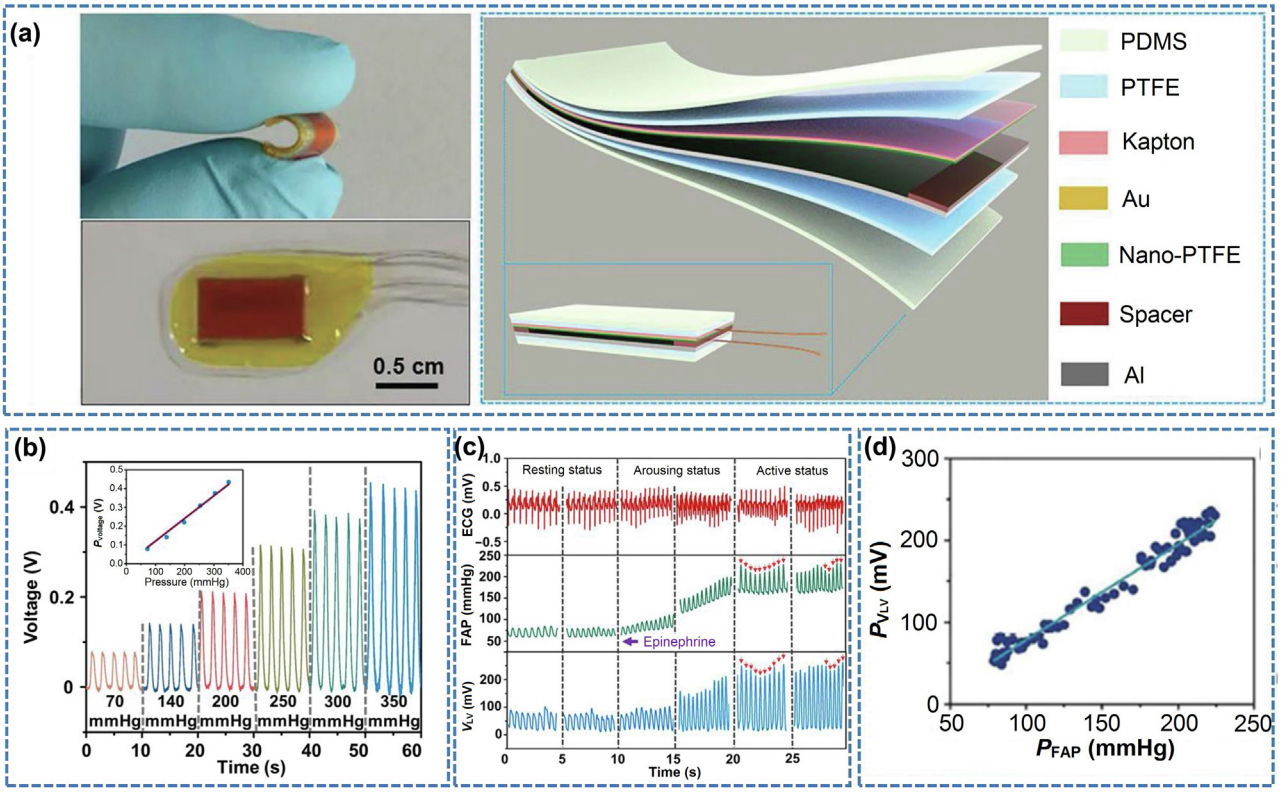

Fig. 3. (Color online) The TENG as a cardiac sensor. (a) Photograph and schematic diagram of the SEPS. (b) V_{oc} of the SEPS under different pressure levels. Inset: the measured results and linear fits of the peak V_{oc} of the SEPS with corresponding pressure peaks. (c) Electrocardiogram (ECG), FAP and SEPS signals at different physical status. (d) Linear correlation between peak V_{oc} of the SEPS and peak FAP. Reprinted with permission from Ref. [41], Copyright © 2018 John Wiley and Sons.

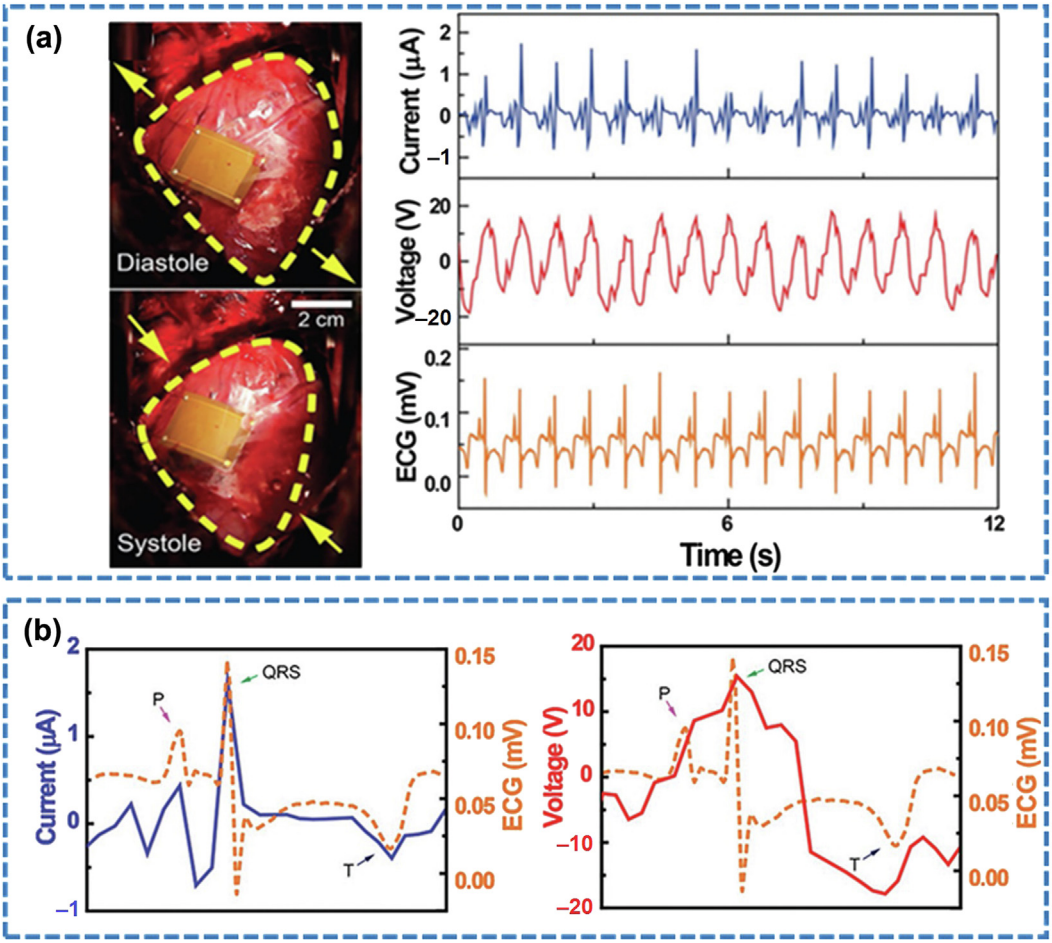

Fig. 4. (Color online) The PENG based cardiac sensor. (a) Photographs of the cardiac sensor. Corresponding output of the device and ECG recorded from porcine heartbeat simultaneously *in vivo*. (b) Magnified view of the ECG, current, and voltage peak. Reprinted with permission from Ref. [33], Copyright © 2017 John Wiley and Sons.

inflammatory reaction through histological effects analysis after implantation for a week. These results indicated the potential application of PENG as a heart monitoring sensor, which could detect cardiac information.

Zheng et al. [30] developed an innovative *in vivo* cardiac sensor which is based on an iTENG. Al film with the thickness of 100 μm was employed as one triboelectric layer, and a nanostructured polytetrafluoroethylene (n-PTFE, 50 μm) thin film, fixed on a flexible Kapton (polyimide) film (150 μm), was used as another triboelectric layer. An ultrathin Au layer (50 nm) on the back side of the Kapton film and Al film formed the electrodes. The iTENG had a keel structure which consisted of a vigorously resilient titanium sheet. A core/shell/shell encapsulating method was used in preparation of the device. PTFE, polydimethylsiloxane (PDMS) and Parylene were sequentially used to achieve the biocompatible, flexible and hermetic packaging (Fig. 5a). The V_{oc} could reach about 90 V and the I_{sc} was about 12 μA before encapsulation. And the I_{sc} and V_{oc} were about 7.5 μA and 45 V after encapsulation, respectively. The iTENG was located between the pericardium and heart in a male adult Yorkshire porcine model (30 kg). The lateral wall of the left ventricular produced the highest output compared to the other implantation sites (Fig. 5b), and the V_{oc} was up to about 14 V *in vivo*, and the I_{sc} was about 5 μA. The V_{oc} and I_{sc} signals kept pace with ECG. How HR and the cardiac contraction influenced the sensor outputs was also investigated. When HR varied from 60 to 120 bpm, the amplitudes of sensor output voltage showed no obvious change. The cardiac contractility of the heart, represented by the systolic blood pressure (sBP), was enhanced by injecting epinephrine. When sBP rose from 105 to 250 mmHg, the sensor voltage increased synchronously from 2 to 6 V. Different heart rates (60, 80, and 120 bpm) modulated by an electronic pacemaker were precisely monitored (R^2 = 0.983) by using a wireless transmission system to transmit and process signals produced by iTENG. The whole system worked well after 72 h of implantation, and the long-term reliability of iTENG was significantly promoted. This study successfully presented a self-powered, wireless cardiac monitoring system.

Ma et al. [32] adopted the design of TENG in the study of Zheng et al., and investigated the real-time biomedical monitoring ability with the self-powered, one-stop and flexible implantable triboelectric active sensor (iTEAS). With a total size of 30 mm × 20 mm × 1 mm, the iTEAS was inserted into the space between pericardium and epicardium of an adult Yorkshire pig (30 kg), and fixed onto the pericardium. The V_{oc} and I_{sc} of iTEAS could reach to 10 V and 4 μA *in vivo*. Thereinto, the voltage signals were highly synchronous to corresponding ECGs. HR_{iTEAS} (HR measured by the iTEAS) was highly consistent with HR_{ECG} (HR measured by ECG), with an accuracy of about 99%. The synchronicity between R waves and peak voltages of iTEAS persisted under resting, active and stressed states. Cardiac arrhythmias, such as ventricular premature contraction and atrial fibrillation, could be monitored in real-time. The same stable periodical fluctuations were observed between the respiration and the peak output voltages of the iTEAS at lateral walls (right lateral wall and left lateral wall) of heart (Fig. 5c). The respiratory rate calculated based on maximal peak to maximal peak interval of iTEAS voltage output

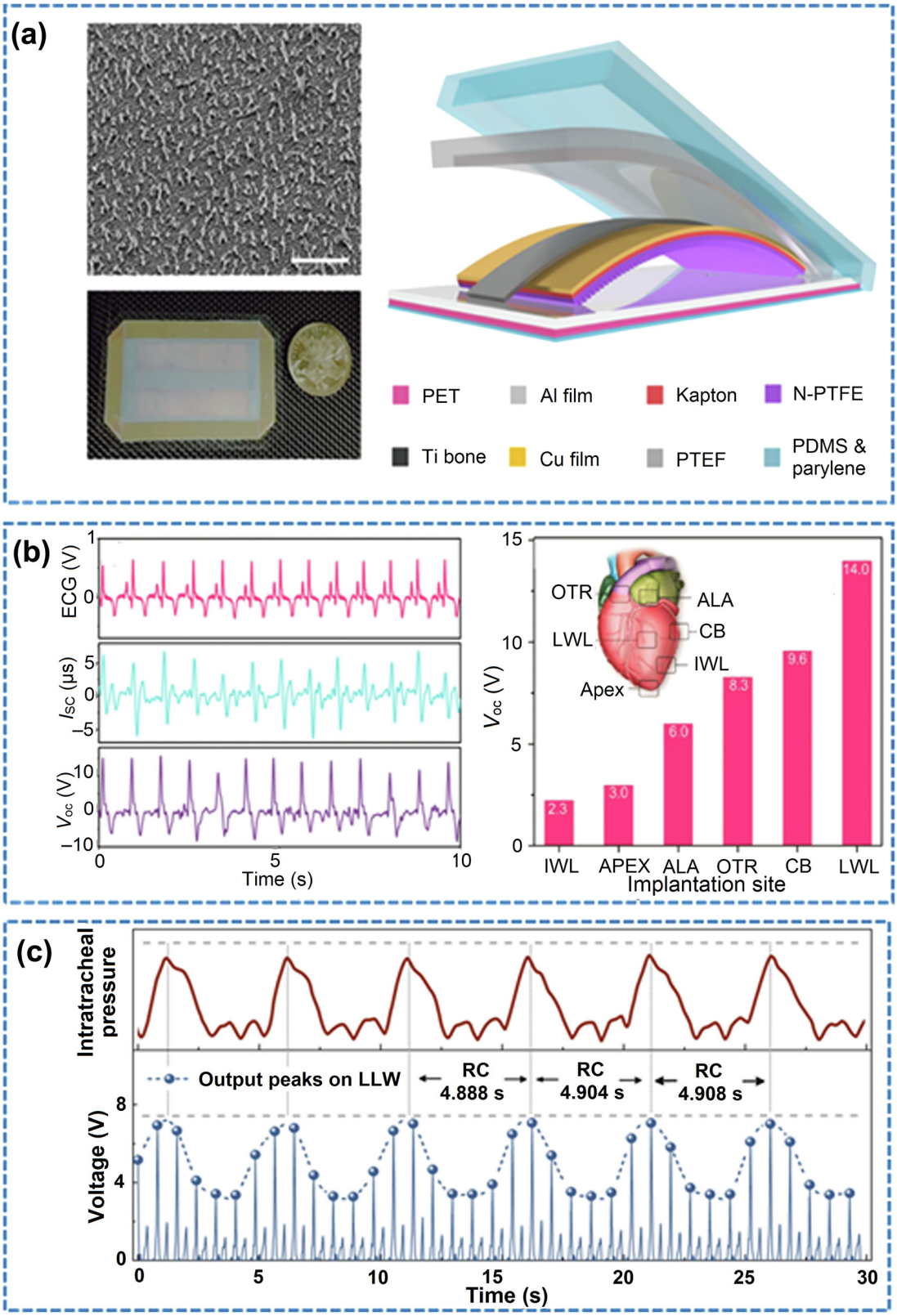

Fig. 5. (Color online) The iTENG based cardiac sensor. (a) The photograph and schematic diagram of the cardiac sensor. (b) ECG and corresponding electric output of the iTENG *in vivo* along with the output of the iTENG at different implant sites (IWL, the inferior wall of the left ventricular; ALA, the auricle of the left atrium; OTR, the right ventricular; CB, the cardiac base; LWL, the lateral wall of the left ventricular). Reprinted with permission from Ref. [30], Copyright © 2016 American Chemical Society. (c) The voltage peaks fluctuated stably and periodically as the iTEAS was anchored over the left lateral wall (LLW) [32]. Reprinted with permission from Ref. [32], Copyright © 2016 American Chemical Society.

was coordinated with the ventilating rate controlled by an artificial respirator. In addition, the sBP had a correlation with the output voltage of iTEAS, and the pressure and velocity of blood flow could be estimated. Two weeks after implantation, the encapsulated device was intact, with no corrosion or rupture in the complicated *in vivo* environment. Infiltration of lymphocytes was not detected at the implantation site in the myocardium tissues. These results presented the promising application of iTEAS to monitor real-time various physiological signals *in vivo*.

3.2. Respiration sensor

Zheng et al. [29] developed an iTENG which could harvest the periodic breathing energy *in vivo* for the first time, and then power a pacemaker prototype. A PDMS film (100 μm) with pyramid arrays on the surface and an Al foil acted as the two triboelectric layers. Two flexible spacers (400 μm) were set to separate the triboelectric layers. The PDMS was fixed on a Kapton film with a thickness of 30 μm which served as the substrate. Au film on the back of Kapton and Al foil worked as the two electrodes. The whole device was totally packaged by PDMS (50 μm) (Fig. 6a). The flexible device with PDMS, Kapton and Al foil based iTENG could easily sense the breathing *in vivo* after it was implanted into the left chest skin of the rat (Fig. 6b). The overall size was 1.2 cm × 1.2 cm × 0.2 cm, but the working area of the iTENG was only 0.8 cm × 0.8 cm due to the spacer structure. The I_{sc} and V_{oc} were about 0.25 μA and 12 V before implantation respectively. The values of *in vivo* generated electricity become 0.14 μA and 3.73 V, respectively (Fig. 6c). There were about 50 "paired peak groups" per minute in iTENG electrical outputs, which was in accordance with the breathing rate controlled by a respirator. In the typical forced vital capacity (FVC) curve, the ratio between the peak values of positive and negative current pulses were the same as that between inspiratory reserve volume (IRV) and expiratory reserve volume (ERV) (Fig. 6d). Besides, the iTENG showed the same shape of the short-circuit current with the FVC curve, demonstrating the feasibility of iTENG based respiration sensor *in vivo*.

3.3. Blood pressure sensor

Zhang et al. [19] developed a PENG which could harvest pulse energy of an ascending aorta. The PENG included a flexible PVDF thin film covered by Al layer, and encapsulated by polyimide (PI) film (50 μm). Through an intra-aortic balloon pump driving saline in a latex tube to simulate the pump function of heart, the output current and voltage were proportional to the changing rate of the flow pressure (FP) and the size of the PVDF film. The PVDF film of 2.5 cm × 5.6 cm × 200 μm based PENG could output a max current of 400 nA and voltage of 10.3 V under the FP of 160/80 mmHg. The packaged device with the same size was implanted to wrap around the ascending aorta in a male domestic porcine (30 kg). The current peak was 300 nA and voltage peak was 1.5 V with a duration of 350 ms respectively *in vivo*. These output electrical signals were highly synchronous to the HR, BP and ECG signals. This

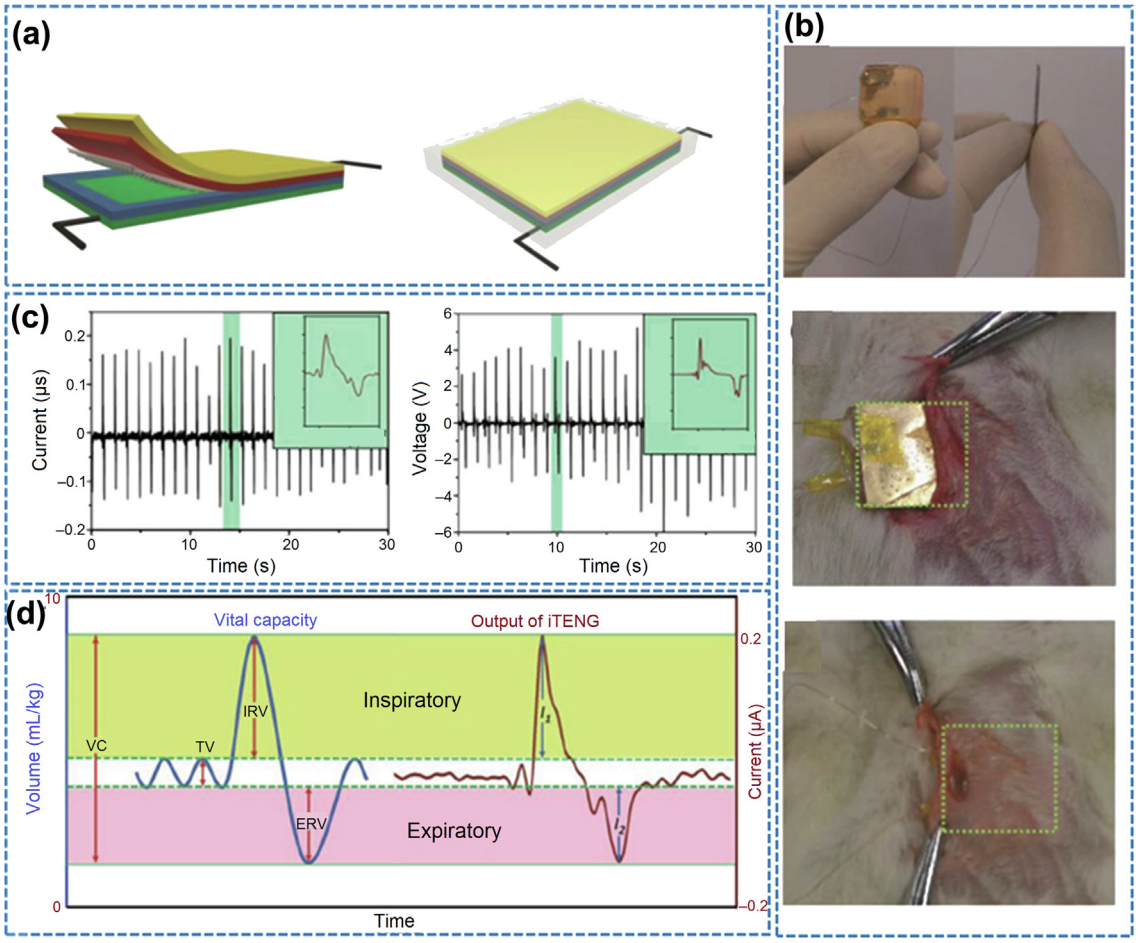

Fig. 6. (Color online) The iTENG based respiration sensor. (a) The photograph and schematic diagram of the respiration sensor. (b) Photograph of an iTENG implanted under the chest skin. (c) The I_{sc} and V_{oc} of the iTENG *in vivo*. (d) Relationship between respiration and short-circuit of the sensor. Reprinted with permission from Ref. [29], Copyright © 2014 John Wiley and Sons.

study firstly tried to harvest ascending aorta's pulse biomechanical energy, and proved the possibility of this implantable PENG as an active BP sensor *in vivo*.

Inspired by the previous study, Cheng et al. [42] investigated a piezoelectric thin film (PETF) based PENG as a self-powered BP sensor by adopting the design of PENG in the study of Zhang et al. (Fig. 7a). Through an intra-aortic balloon pump driving saline in a latex tube test *in vitro*, the maximal output was gained when the tightness, that is the ratio of the PETF length to the perimeter of latex tube, was 90%. The peak voltage showed a high-sensitivity of 173 mV/mmHg and excellent linearity with peak flow pressure ($R^2 > 0.99$). The device showed excellent stability of more than 50,000 operating cycles, and achieved a maximal instantaneous power of 2.3 μW, which was favorable for long-time use *in vivo*. The encapsulated device was implanted to wrap around the ascending aorta in a male Yorkshire porcine (~50 kg) with a tightness of 90%. There was a favorable linearity ($R^2 = 0.971$) with a sensitivity of 14.3 mV/mmHg between the measured output voltage peak and the systolic BP peak (Fig. 7b). A maximal instantaneous power of 40 nW was obtained. This work presented a self-powered BP monitoring system, which could monitor real-time BP and gave real-time alarm.

3.4. Gastrointestinal sensor

Dagdeviren et al. [40] invented a piezoelectric system based on PZT ribbons which could sense the gastrointestinal (GI) pressure and motility. Poly(pyromellitic dianhydride-*co*-4,40-oxydianiline) amic acid solution (PI) with a layer thickness of 1.2 μm and ultraviolet curable epoxy with a layer thickness of 10 μm were sequentially used to encapsulate the device to provide protection and isolation from the GI environment (Fig. 8a). The encapsulated device kept mechanically stable after 48 h-immersion in simulated gastric and intestinal fluid. The voltage output presented negligible changes after 10,000 repeated bending cycles. Cell cytotoxicity analyses proved the good biocompatibility of the device. The

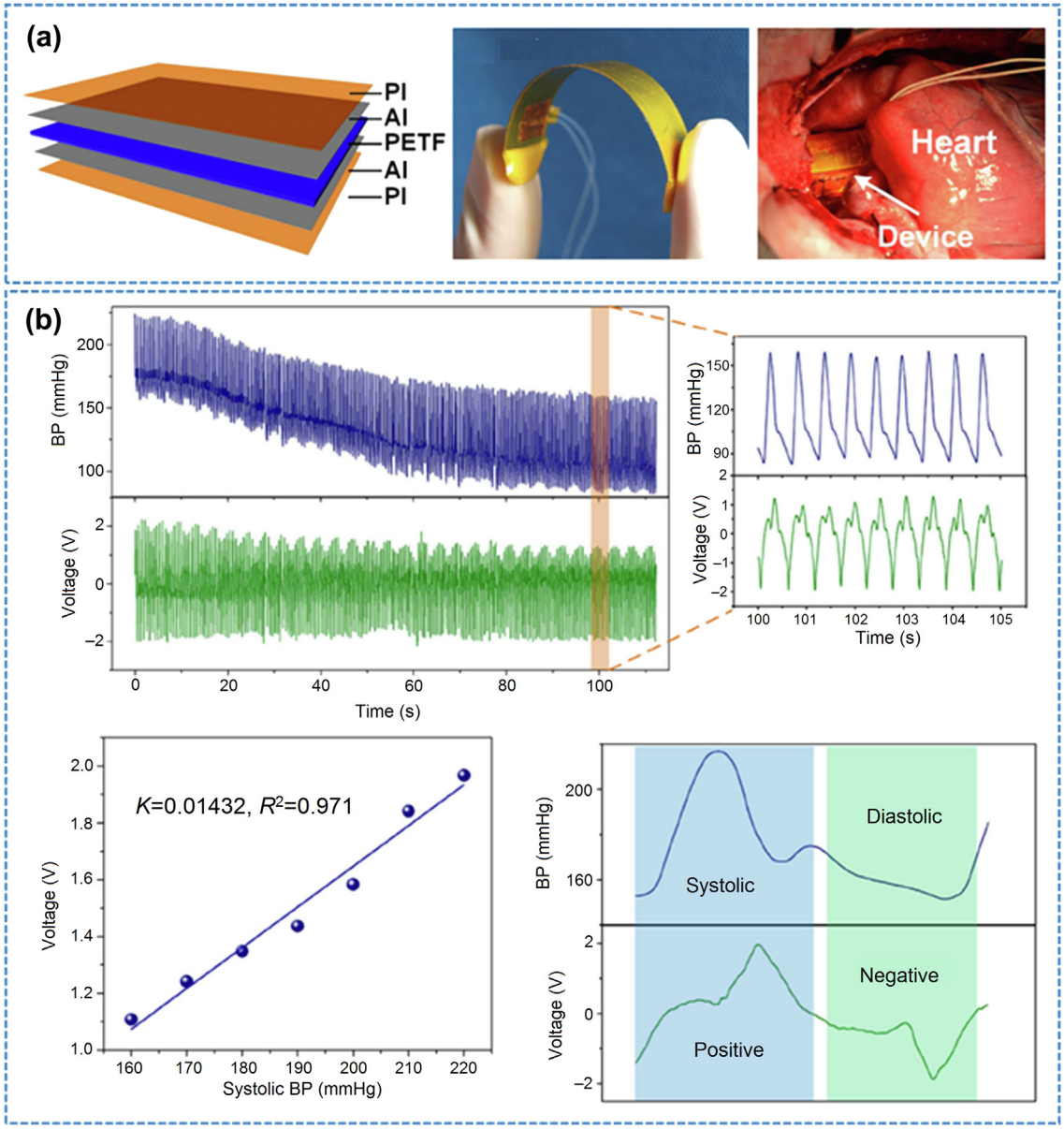

Fig. 7. (Color online) The PENG as a BP sensor. (a) The schematic diagram of the PENG which was flexible enough to wrap on the ascending aorta of porcine; (b) The *in vivo* output voltage of the BP sensor which had an excellent correlation with different systolic BP. Reprinted with permission from Ref. [42], Copyright © 2016 Elsevier.

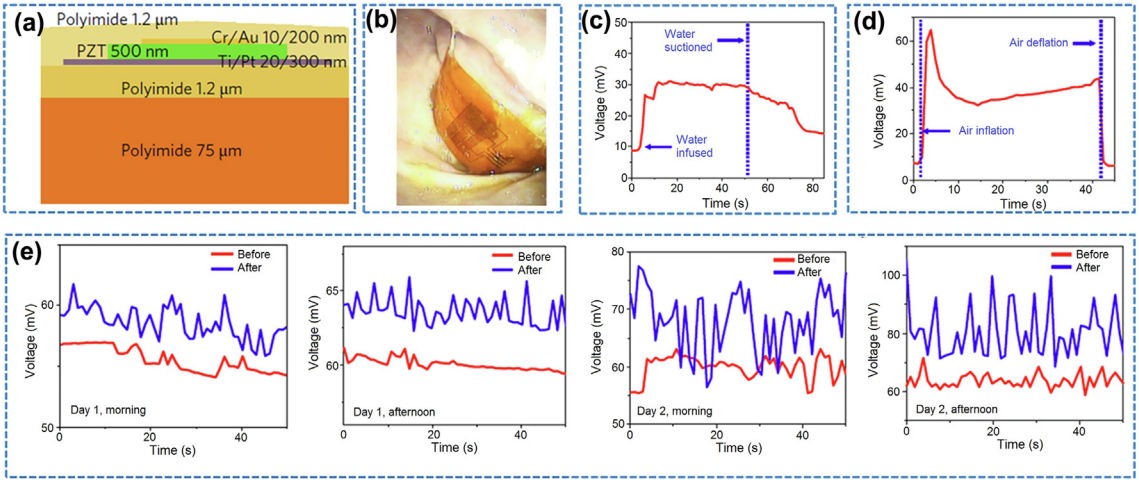

Fig. 8. (Color online) The PENG as a gastrointestinal sensor. (a) Cross-sectional structure of the PZT based PENG. (b) Photographs of the GI sensor on the wall of the stomach during inflation. (c) Representative real-time voltage output for a cycle of water infusion and suction. (d) Representative real-time voltage output of a cycle of air inflation and deflation. (e) Real time voltage output graphs before and after milk ingestion. Reprinted with permission from Ref. [40], Copyright © 2017 Springer Nature.

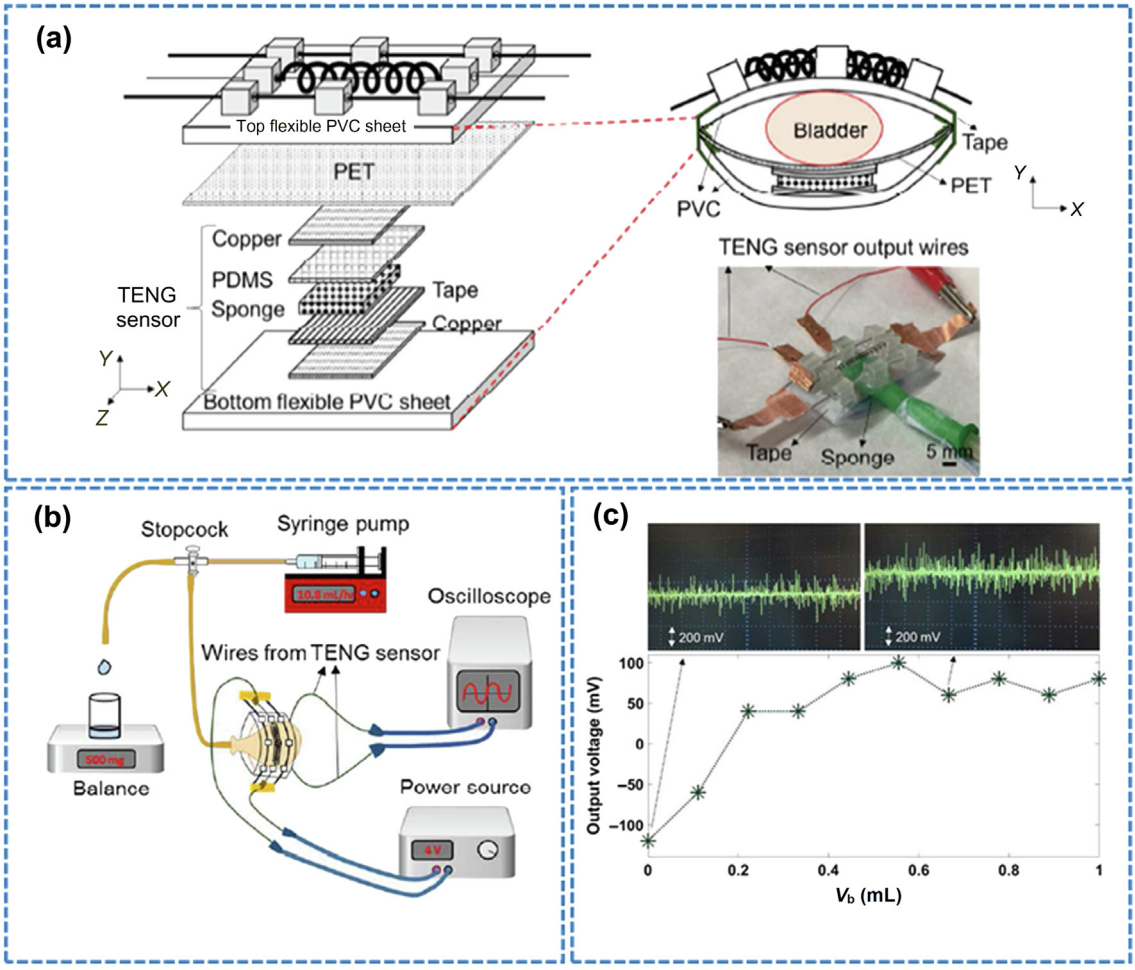

Fig. 9. (Color online) The TENG working as a bladder sensor. (a) Structure of the bladder sensor. (b) The benchtop experiment of the TENG sensor integrated BMA. (c) The *in vivo* test of the bladder sensor. Reprinted with permission from Ref. [43], Copyright © 2018 American Chemical Society.

encapsulated device could sense the inner pressure of stomach via *in vitro*, *ex vivo* and *in vivo* experiment validation. When the device was settle on the stomach lining in a Yorkshire swine of around 45 kg (Fig. 8b), the voltage output incrementally varied from 8 to 30 mV when 200 mL water was infused into the stomach, and decreased to around 15 mV after the water was suctioned (Fig. 8c). The generated voltage increased from about 10 mV to 60 mV when the air was introduced into the stomach, remained

at the plateau voltage level during the 40-s inflation period, and decreased to the baseline level after the air was released (Fig. 8d). To prove the capacity of the sensor in monitoring GI motility, the device was implanted in the gastric cavity of an awake and ambulating Yorkshire swine. The voltage output for morning and afternoon trials increased after milk ingestion (Fig. 8e). These results showed that the encapsulated self-powered sensor exhibited mechanical and electrical robustness in the environment of stomach, and could sensor the inner pressure and motility of the stomach.

3.5. Bladdar sensor

Lee and co-workers [43] invented a wet sponge-based TENG bladder sensor integrated with a bi-stable micro-actuator (BMA) which could monitor the fullness of bladder and then activate the BMA to void it. A PET film (50 μm) was joined with a polyvinyl chloride (PVC) sheet using the tape (50 μm). Two cooper electrodes with 1.4 cm × 2.2 cm were fixed on the center of PVC sheet and the polyethylene terephthalate (PET) layer respectively. A sponge (1 mm) containing 0.2 mL of DI water and a PDMS (431.8 μm) with the size of 1.4 cm × 2.2 cm were set between the copper electrodes (Fig. 9a). The voltage of TENG sensor increased from 35.6 to 114 mV by increasing the external force from 0 to 6.86 N. The group tested the integrated TENG sensor with the actuator using the benchtop setup *in vitro* (Fig. 9b). The output voltage of the integrated TENG sensor showed sinusoida-like signal and increased when the balloon acting as bladder was filled continually. The *in vivo* test also showed the output voltage increased by adding the saline volume of bladder (V_b) and started to saturate at about V_b = 0.67 mL (Fig. 9c). This work presented the promising application of TENG to monitor the bladder pressure and state *in vivo*.

4. Discussion and conclusions

Plenty of energy sources in the body can be used to power healthcare electronics, especially IEMDs. There are many ways to harvest these energies, including physical methods such as NGs based on the piezoelectric/triboelectric effect and automatic wristwatches, and the chemical methods like biofuel cells. This review focuses on the NGs based on the piezoelectric/triboelectric effect and their applications as biomedical sensors *in vivo*, and the researches are summarized in Table 1. The material property is very important to the device performance. The materials chosen in recent PENG-based biomedical sensors were inorganic PZT and PMN-PZT-Mn and organic PVDF, which have excellent piezoelectric effect. The most commonly used friction materials of TENGs in the biomedical sensors were PTFE and Al film, which have different electron binding capacity. The flexible NGs were tiled and fixed on the heart, gastrointestinal tract, bladder, or wrapped around the blood vessels, then the expansion and contraction of these organs could extrude the devices periodically, transferring the mechanical energy into electric signals.

NGs can obtain vital physiological information by analyzing the output electrical signals. This article reviews the exploration and application of NGs as the cardiac sensor, respiration sensor, blood pressure sensor, gastrointestinal sensor and bladder sensor. The self-powered sensors have unique advantages over traditional sensors. Especially when implanted into the body, self-powered sensors can monitor the physiological and pathological information with high fidelity and accuracy without artifacts induced by subjects. Although NG is still in their infancy as a biomedical sensor, these studies have achieved inspiring results. In order to maximize the role of the self-powered sensors in healthcare, there is still a lot of work to be done. First of all, the optimal implantation site should be identified for the measured biomedical parameter. For example, the cardiac sensor based on TENG, in the study of Zheng et al., produced the maximal electrical outputs at the lateral wall of the left ventricular compared to other four implantation sites. The optimal implantation site can improve the signal to noise ratio for biomedical signals, benefit the wireless transmission of physiological signals, and provide a greater possibility for long-term *in vivo* implantation. The second challenge is the encapsulation and long-term reliability of NGs. The NGs should have good biocompatibility, and should not leak in the moist *in vivo* environment or under long-term extrusion to maintain efficient output. Most studies reviewed above showed good biocompatibility for *in vivo* tests,

Table 1
A summary of various NG-based sensors *in vivo*.

Sensor type	NG	Materials	Output *in vivo* (implantation site)	Type	Refs.
Cardiac sensor	PENG	PMN-PZT-Mn	V_{oc}: 17.8 V, I_{sc}: 1.75 μA (epicardium)	Heart rate, characteristic waves in ECG	[33]
	TENG	n-PTFE thin film/Al film	V_{oc}: ~14 V, I_{sc}: ~5 μA (LWL)	Heart rate (R^2 = 0.983)	[29]
	TENG	n-PTFE thin film/Al film	V_{oc}: 10 V, I_{sc}: 4 μA (pericardium)	Heart rate, respiration rate, BP, velocity of blood flow	[32]
	TENG	n-PTFE film/Al foil	V_{oc}: ~80 mV (left ventricle), V_{oc}: ~ 8 mV (left atrial)	P_{FAP}, P_{LAP}	[41]
Respiration sensor	TENG	PDMS/Al/Kapton	V_{oc}: 3.73 V, I_{sc}: 0.14 μA (chest skin)	Respiration rate	[29]
Blood pressure sensor	PENG	PVDF thin film	V_{oc}: 1.5 V, I_{sc}: 300 nA (ascending aorta)	Heart rate, BP	[19]
	PENG	PVDF thin film	Power: 40 nW (ascending aorta)	BP (R^2 = 0.971)	[42]
Gastrointestinal sensor	PENG	PZT ribbons	V_{oc} :~8 mV (stomach lining)	Inner pressure, gastrointestinal motility	[40]
Bladder Sensor	TENG	PDMS/PET/PVC	V_{oc} :114 mV (around bladder)	Bladder pressure	[43]

but the duration for *in vivo* tests was relatively short when comparing with the practical need for IEMDs. Stable NG outputs are the foundation for the relationship with physiological information, and more researches are needed to further promote the long-term reliability of NGs. Finally, since most studies above just observed that the self-powered sensors' output signals kept pace with the physiological information, this suggests a huge space for establishing a model to describe the relationship between the sensor output and the physiological signals as accurately as possible.

PENG and TENG with different characteristics are widely used in biomedical application, while they have both advantages and disadvantages. TENGs have wide selection of materials. Fundamentally, all materials with different electrons binding ability can be utilized to make a TENG, thus, biocompatibility for TENGs is easy to achieve. However, PENGs can only choose limited piezoelectric materials. The working mode of PENG is based on the relative movement of friction layers, while that of TENG is on account of shape change. In this regards, PENG have better encapsulation strategy than TENG, and smaller device size can be obtained. For PENG, the materials chosen are with higher toxicity to cells and tissues, thus, biocompatible materials are required in the future application. In addition, the PENGs should be made flexibly to fit for the organs as closely as possible, which is more adaptable for patients. Finally, the output of PENG needs to be enhanced for long-term application. Based on the differentiated signal demand of specific medical applications, TENG with high voltage and low current output and PENG with low voltage and high current output are flexible to be employed.

At present, NGs have practical applications in a variety of fields as sensors, such as motion sensing, security check, gas sensing and so on. The development of self-powered sensors is currently booming and the NGs can be potentially used in intracranial pressure sensor, intraocular pressure sensor, intravascular pressure sensor and intramedullary press sensor. In the medical field, the self-powered sensor may promote the development of next-generation implantable biomedical sensors for monitoring and diagnosis of many diseases, such as cardiovascular diseases [44]. Besides self-powered sensors, NGs have also been used in pacemakers and stimulators for the deep brain, nerves, or bone [45], and bioabsorbable NGs have also been developed [46], which open new routes for the development of healthcare electronics.

Conflict of interest

The authors declare that they have no conflict of interest.

Acknowledgments

This work was supported by the National Key Research and Development Program of China (2016YFA0202703), the Scientific Research Foundation for Advanced Scholars of Foshan University (Gg07136, Gg07164), the Key Platform and Scientific Research Project of Guangdong Provincial Education Department (2018KTSCX246), the Science and Technology Planning Project of Guangdong Province (2018B030331001), the National Natural Science Foundation of China (61875015, 31571006, 81570202, and 8157037), the Beijing Natural Science Foundation (2182091), and the National Youth Talent Support Program.

Author contributions

Jinyan Sun, AnPing Yang, Chaochao Zhao, and Zhou Li proposed conceptualization. Jinyan Sun and Chaochao Zhao investigated the relate work. Jinyan Sun and Chaochao Zhao prepared the original draft. AnPing Yang, Fang Liu, and Zhou Li wrote the review. Zhou Li supervised the manuscript.

Appendix A. Supplementary data

Supplementary data to this article can be found online at https://doi.org/10.1016/j.scib.2019.07.001.

References

[1] Zurlo G, Zhang Q. The history of oxygen sensing: 2016 lasker award for basic medical research. Sci Bull 2016;61:1665–8.
[2] Wang C, Li YQ, Liao Y, et al. 2018 Chinese pediatric cardiology society (cpcs) guideline for diagnosis and treatment of syncope in children and adolescents. Sci Bull 2018;63:1558–64.
[3] Xu YL, Zhang XH, Zhu SY, et al. Multi-type sensor placement and response reconstruction for structural health monitoring of long-span suspension bridges. Sci Bull 2016;61:313–29.
[4] Barold SS. Wilson Greatbatch (1919–2011). J Interventional Cardiac Electrophys 2012;33:259–60.
[5] Beck H, Boden WE, Patibandla S, et al. 50th anniversary of the first successful permanent pacemaker implantation in the united states: historical review and future directions. Am J Cardiol 2010;106:810–8.
[6] Potter MC. Electrical effects accompanying the decomposition of organic compounds. II. Ionisation of the gases produced during fermentation. Proc R Soc Lond B Conta 1915;89:96.
[7] Yahiro AT, Lee SM, Kimble DO, Bioelectrochemistry I. enzyme utilizing bio-fuel cell studies. Biochim Biophys Acta 1964;88:375–83.
[8] Ko WH, Hynecek J. Implant evaluation of a nuclear-power source-betacel battery. IEEE T Bio-Med Eng 1974;Bm21:238–41.
[9] Furman S. Nuclear pacemakers. Pace 1979;2:135–6.
[10] Parsonnet V, Myers GH, Gilbert L, et al. Clinical experience with nuclear pacemakers. Surgery 1975;78:776–86.
[11] Mond HG, Proclemer A. The 11th world survey of cardiac pacing and implantable cardioverter-defibrillators: calendar year 2009-A world society of arrhythmia's project. Pace 2011;34:1013–27.
[12] Shi BJ, Li Z, Fan YB. Implantable energy-harvesting devices. Adv Mater 2018;30:e1801511.
[13] Zheng Q, Shi BJ, Li Z, et al. Recent progress on piezoelectric and triboelectric energy harvesters in biomedical systems. Adv Sci 2017;4:1700029.
[14] Guo HY, Yeh MH, Lai YC, et al. All-in-one shape-adaptive self-charging power package for wearable electronics. ACS Nano 2016;10:10580–8.
[15] Xu S, Qin Y, Xu C, et al. Self-powered nanowire devices. Nat Nanotechnol 2010;5:366–73.
[16] Wang ZL, Song JH. Piezoelectric nanogenerators based on zinc oxide nanowire arrays. Science 2006;312:242–6.
[17] Fan FR, Tian ZQ, Wang ZL. Flexible triboelectric generator! Nano Energy 2012;1:328–34.
[18] Yang PK, Lin L, Yi F, et al. A flexible, stretchable and shape-adaptive approach for versatile energy conversion and self-powered biomedical monitoring. Adv Mater 2015;27:3817–24.
[19] Zhang H, Zhang XS, Cheng XL, et al. A flexible and implantable piezoelectric generator harvesting energy from the pulsation of ascending aorta: in vitro and *in vivo* studies. Nano Energy 2015;12:296–304.
[20] Pi ZY, Zhang JW, Wen CY, et al. Flexible piezoelectric nanogenerator made of poly(vinylidenefluoride-*co*-trifluoroethylene) (PVDF-TRFE) thin film. Nano Energy 2014;7:33–41.
[21] Park DY, Joe DJ, Kim DH, et al. Self-powered real-time arterial pulse monitoring using ultrathin epidermal piezoelectric sensors. Adv Mater 2017;29:1702308.
[22] Jeong CK, Han JH, Palneedi H, et al. Comprehensive biocompatibility of nontoxic and high-output flexible energy harvester using lead-free piezoceramic thin film. APL Mater 2017;5:074102.
[23] Hwang GT, Yang J, Yang SH, et al. A reconfigurable rectified flexible energy harvester via solid-state single crystal grown PMN-PZT. Adv Energy Mater 2015;5:1500051.
[24] Ouyang H, Tian JJ, Sun GL, et al. Self-powered pulse sensor for antidiastole of cardiovascular disease. Adv Mater 2017;29:1703456.
[25] Kim S, Gupta MK, Lee KY, et al. Transparent flexible graphene triboelectric nanogenerators. Adv Mater 2014;26:3918–25.
[26] Zi YL, Lin L, Wang J, et al. Triboelectric-pyroelectric-piezoelectric hybrid cell for high-efficiency energy-harvesting and self-powered sensing. Adv Mater 2015;27:2340–7.
[27] Hu W, Wei X, Zhu L, et al. Enhancing proliferation and migration of fibroblast cells by electric stimulation based on triboelectric nanogenerator. Nano Energy 2019;57:600–7.
[28] Li Z, Zhu GA, Yang RS, et al. Muscle-driven *in vivo* nanogenerator. Adv Mater 2010;22:2534–7.
[29] Zheng Q, Shi BJ, Fan FR, et al. *In vivo* powering of pacemaker by breathing-driven implanted triboelectric nanogenerator. Adv Mater 2014;26:5851–6.
[30] Zheng Q, Zhang H, Shi BJ, et al. *In vivo* self-powered wireless cardiac monitoring via implantable triboelectric nanogenerator. ACS Nano 2016;10:6510–8.

[31] Zhao C, Feng H, Zhang L, et al. Highly efficient *in vivo* cancer therapy by an implantable magnet triboelectric nanogenerator. Adv Funct Mater 2019;1808640.
[32] Ma Y, Zheng Q, Liu Y, et al. Self-powered, one-stop, and multifunctional implantable triboelectric active sensor for real-time biomedical monitoring. Nano Lett 2016;16:6042–51.
[33] Kim DH, Shin HJ, Lee H, et al. *In vivo* self-powered wireless transmission using biocompatible flexible energy harvesters. Adv Funct Mater 2017;27:1700341.
[34] Wang ZL. On Maxwell's displacement current for energy and sensors: the origin of nanogenerators. Mater Today 2017;20:74–82.
[35] Shao JJ, Willatzen M, Jiang T, et al. Quantifying the power output and structural figure-of-merits of triboelectric nanogenerators in a charging system starting from the Maxwe's displacement current. Nano Energy 2019;59:380–9.
[36] Gao ZY, Zhou J, Gu YD, et al. Effects of piezoelectric potential on the transport characteristics of metal-zno nanowire-metal field effect transistor. J Appl Phys 2009;105:113707.
[37] Wang ZL, Chen J, Lin L. Progress in triboelectric nanogenerators as a new energy technology and self-powered sensors. Energy Environ Sci 2015;8:2250–82.
[38] Zhang XS, Han M, Kim B, et al. All-in-one self-powered flexible microsystems based on triboelectric nanogenerators. Nano Energy 2018;47:410–26.
[39] Dagdeviren C, Yang BD, Su YW, et al. Conformal piezoelectric energy harvesting and storage from motions of the heart, lung, and diaphragm. Proc Natl Acad Sci USA 2014;111:1927–32.
[40] Dagdeviren C, Javid F, Joe P, et al. Flexible piezoelectric devices for gastrointestinal motility sensing. Nat Biomed Eng 2017;1:807–17.
[41] Liu Z, Ma Y, Ouyang H, et al. Transcatheter self-powered ultrasensitive endocardial pressure sensor. Adv Funct Mater 2018;1807560.
[42] Cheng X, Xue X, Ma Y, et al. Implantable and self-powered blood pressure monitoring based on a piezoelectric thinfilm: simulated, *in vitro* and *in vivo* studies. Nano Energy 2016;22:453–60.
[43] Hassani FA, Mogan RP, Gammad GG, et al. Toward self-control systems for neurogenic underactive bladder: a triboelectric nanogenerator sensor integrated with a bistable micro-actuator. ACS Nano 2018;12:3487–501.
[44] Wan BS, Guo SQ, Sun JC, et al. Investigating the interlayer electron transport and its influence on the whole electric properties of black phosphorus. Sci Bull 2019;64:254–60.
[45] Feng H, Zhao C, Tan P, et al. Nanogenerator for biomedical applications. Adv Healthc Mater 2018;7:e1701298.
[46] Jiang W, Li H, Liu Z, et al. Fully bioabsorbable natural-materials-based triboelectric nanogenerators. Adv Mater 2018;30:e1801895.

Jinyan Sun received her Bachelor's Degree in Shandong University in 2008, and Doctor's Degree in Huazhong University of Science and Technology of 2013. She is currently a researcher of Department of Biomedical Engineering in Foshan University. Her research work mainly focuses on *in vivo* self-powered biosensors and human brain function with near-infrared spectroscopy and electroencephalography.

Zhou Li received his Bachelor's Degree from Wuhan University in 2004, and Doctor's Degree from Peking University in Department of Biomedical Engineering in 2010. He joined School of Biological Science and Medical Engineering of Beihang University in 2010 as an associate Professor. Currently, he is a Professor in Beijing Institute of Nanoenergy and Nanosystems, Chinese Academy of Sciences. His research interests include nanogenerators, *in vivo* energy harvesters and self-powered medical devices, biosensors.